Origin of the large interfacial perpendicular magnetic anisotropy in MgO/Co_{2}FeAl

Sicong Jiang, Safdar Nazir, and Kesong Yang

Phys. Rev. B **101**, 134405 — Published 6 April 2020

DOI: 10.1103/PhysRevB.101.134405

Origin of the large interfacial perpendicular magnetic anisotropy in MgO/Co_2FeAl

Sicong Jiang,[1,2] Safdar Nazir,[1] and Kesong Yang[1,2,3,*]

[1] *Department of NanoEngineering and Program of Chemical Engineering, University of California San Diego, La Jolla, California 92093-0448, USA*
[2] *Program of Materials Science and Engineering, University of California San Diego, La Jolla, California 92093-0418, USA*
[3] *Center for Memory and Recording Research, University of California San Diego, La Jolla, California 92093-0401, USA*

Interfacial perpendicular magnetic anisotropy in the MgO/Co_2FeAl heterostructure is desired for technological applications, while its origin of the large interfacial anisotropy constant (K_i) remains controversial. Here we show that, by modeling four types of interface models for MgO/Co_2FeAl system using first-principles calculations, the MgO/Co_2 interface is energetically more favorable than MgO/FeAl interface, and the interfacial Co atoms at the former interface produce out-of-plane K_i while the interfacial Fe atoms at the later interface produce in-plane K_i. The origin of this different behavior can be explained from the atomic-resolved and orbital-resolved K_i along with the perturbation theory energy analysis. In addition, we also studied the influence of 26 capping layers on the interfacial magnetic anisotropy of MgO/Co_2FeAl and found that Fe- and W-capping can significantly enhance the K_i in the MgO/Co_2FeAl with a particularly large K_i of 4.90 mJ/m^2 in the W-capped model. This work clarifies the atomistic origin of the interfacial perpendicular magnetic anisotropy and provides guidance to further enhance interfacial K_i by adding capping layers in the MgO/Co_2FeAl.

I. INTRODUCTION

Magnetic tunnel junctions (MTJs) consisting of two ferromagnetic (FM) layers separated by a thin insulating barrier are core components in spin-transfer-torque magnetic random-access memory (STT-MRAM).[1,2] In particular, the perpendicular MTJs (p-MTJs) that possessed perpendicular magnetic anisotropy (PMA) have attracted great attention in recent years because of their promising applications in the next-generation spintronic devices towards using faster and smaller magnetic bits.[3–6] In p-MTJs, PMA occurs at the interface between ferromagnetic thin film and insulating barrier and its strength is characterized by the magnetic anisotropy constant (K_i), which is defined as the anisotropy energy per unit area.[7] To achieve a high thermal stability of the relative magnetization orientation of the two ferromagnetic electrodes, a large K_i is desired. As p-MTJs shrink to the nanometer scale, a larger K_i is necessary to sustain a sufficient thermal stability. A recent theoretical calculation indicated that a K_i of 4.7 mJ/m^2 is needed for a data retention time of ten years when the memory devices scale down to 10 nm.[8]

PMA has been traditionally achieved at interfaces between ferromagnetic and nonmagnetic heavy metals such as Co/Pt, however, their K_i is small (less than 1 mJ/m^2).[9] In 2010, a large K_i of 1.3 mJ/m^2 was reported at MgO/CoFeB interface, and the MTJ based on this material interface exhibits a high tunnel magnetoresistance ratio of 120% and a low switching current of about 49 μA.[5] Since then, great research efforts have been made either to tune K_i at MgO/Fe interface[7] or to explore the possibility of producing large K_i at novel MgO-based interfaces.[10,11] Co_2FeAl, one prototype compound of full Heusler family, has received increasing interests as one possible alternative to Fe and CoFeB in the MgO-based p-MTJs in recent years because of its excellent properties including high spin polarization,[12] low magnetic damping constant (about 0.001),[13] and small lattice mismatch[14] between Co_2FeAl film and MgO substrate (∼4 %). The magnetic anisotropy at MgO/Co_2FeAl interface was first reported in 2011 and was found very sensitive to the annealing.[10,11,15] Jiang's team[15] and Inomata's team[10] both reported a PMA at MgO/Co_2FeAl interface, independently, and found a magnetic anisotropy transition from in-plane to out-of-plane after annealing.[10] In contrast, in-plane magnetic anisotropy was also found at MgO/Co_2FeAl interface and showed different behavior with the annealing temperature.[11,16] A very recent experimental study also reported an evolution of the PMA at the interface between MgO and Co_2FeAl, *i.e.*, a K_i of zero for as-deposited samples and a K_i of 1.14 (2.01) mJ/m^2 for samples annealed at 320 (450)°C, which is attributed to the modification of the interface during the thermal treatment.[17]

PMA is mainly determined by the magnetic ions of a few monolayers near the interfacial region and there exist two types of interfaces in the MgO/Co_2FeAl heterostructure, *i.e.*, MgO/Co_2 and MgO/FeAl. Accordingly, one may speculate that the different magnetic anisotropy is caused by the different interfacial terminations between MgO substrate and Co_2FeAl film. Inomata's team investigated the PMA at the MgO/Co_2FeAl interface using angular-dependent x-ray magnetic circular dichroism (XMCD), and attributed the PMA mostly to the interfacial Fe atoms at the MgO/FeAl interface.[18] Later, the same team also argued that the PMA at the Co_2FeAl heterostructure is mainly contributed by the large perpendicular orbital magnetic moments of interfacial Fe ions from XMCD measurement.[19] A prior theoretical study indicated that oxygen-top FeAl termination has the highest thermal stability on the basis of density functional theory calculations,[20] which seems to support the above arguments. However, a recent

computational study indicated that FeAl-termination at MgO/Co_2FeAl interface lead to an in-plane instead of out-of-plane magnetic anisotropy, while Co-termination showed the PMA with K_i up to 1.31 mJ/m^2.[21] Therefore, to clarify the atomistic origin of the magnetic anisotropy at the MgO/Co_2FeAl interface, a comprehensive study of the interfacial magnetic properties and evaluation of the relative thermodynamic stability of the two types of materials interfaces are very necessary.

Additionally, a series of recent experimental and computational studies both indicated that metal-based capping layers have a significant influence on the K_i of MgO/Co_2FeAl heterostructure,[22,23] in which capping layers are often used to protect the ferromagnetic layers. For instance, Cr-capped MgO/Co_2FeAl showed an in-plane magnetic anisotropy with a K_i of -0.46 mJ/m^2 while Ta-capped film exhibited a PMA with a K_i of 0.74 mJ/m^2.[22] Gabor *et al* also reported a similar K_i of 0.67 mJ/m^2 in the $Ta/Co_2FeAl/MgO$ multilayers even in the as-deposited state.[23] As a result, adding one capping layer on MgO/Co_2FeAl heterostructure not only protects the ferromagnetic layer but also plays an important role in tuning the K_i. Consequently, a systematic evaluation of the influence of all the possible metal-based capping layers on the K_i of MgO/Co_2FeAl heterostructure is of great importance, and so far, there has been no such a report.

In this research article, we reported a comprehensive study of the interfacial magnetic and energetic properties for the MgO/Co_2FeAl interface without and with capping layers, consisting of two sections. In the first section, we considered four types of MgO/Co_2FeAl models without capping layers, including MgO/Co_2...FeAl, MgO/Co_2...Co_2, MgO/FeAl...Co_2, and MgO/FeAl...FeAl, and investigated their layer-resolved and atomic orbital-resolved K_i and interfacial cleavage energy. In the second section, we systematically investigated the influence of 26 capping layers on the interfacial K_i of the MgO/Co_2...FeAl and MgO/Co_2...Co_2 systems. Our calculations indicate that adding Fe- and W-capping layers can significantly increase the K_i of the system, and particularly, W capping leads to a giant K_i of 4.90 mJ/m^2 in MgO/Co_2...FeAl/W model. This work clarified the atomistic origin of the interfacial perpendicular magnetic anisotropy at MgO/Co_2FeAl, providing some guidance to develop novel p-MTJs with high thermal stability and large K_i.

II. COMPUTATIONAL DETAILS

DFT calculations with spin-orbit coupling (SOC) were carried out using Vienna *Ab-initio* Simulation Package (VASP).[24,25] The projector augmented wave (PAW) pseudopotentials were employed for treating electron-ion interactions,[26] and the generalized gradient approximation (GGA) parameterized by Perdew-Burke-Ernzerhof (PBE) was used for exchange-correction functional.[27]

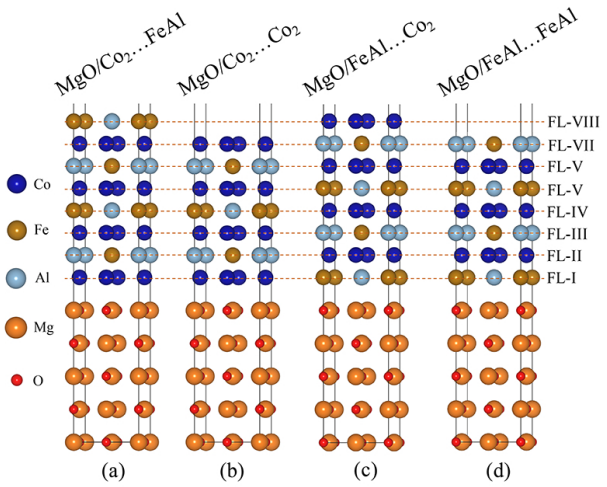

FIG. 1. Schematic crystal structures of uncapped MgO/Co_2FeAl heterostructures. (a) MgO/Co_2 interface with FeAl surface (MgO/Co_2...FeAl), (b) MgO/Co_2 interface with Co_2 surface (MgO/Co_2...Co_2), (c) MgO/FeAl interface with Co_2 surface (MgO/FeAl...Co_2), (d) MgO/FeAl interface with FeAl surface (MgO/FeAl...FeAl).

The cut-off kinetic energy for plane waves was set as 450 eV. Γ-centered k-point grids were set as $6 \times 6 \times 1$ and $21 \times 21 \times 1$ for ionic relaxation and static calculations, respectively, which were determined by a careful convergence test for the perpendicular magnetic anisotropy constant (K_i), total energy, and cleavage energy of the heterostructure models, see Fig. S1 in the Supporting Information.[28] The convergence threshold for electronic self-consistency loop was set to 10^{-6} eV. All the atomic positions and lattice structures were fully relaxed until the residual forces were smaller than 0.02 eV/Å in the structural relaxation. The density of states (DOS) was calculated using the tetrahedron method with Blöchl corrections.[29] The in-plane lattice constant of the MgO/Co_2FeAl heterostructure model was fixed to the lattice constant of MgO (4.215Å).

The K_i was calculated by $(E_{[100]} - E_{[001]})/A$, where $E_{[100]}$ and $E_{[001]}$ represent total energy with magnetization along [100] and [001] direction in a fully self-consistent-field manner, respectively, and A is the in-plane area. It is realized that another approach, *i.e.*, a so-called "force theorem", can also be used to calculate K_i, in which a fully self-consistent collinear calculation is required as the first step. After that, non-collinear calculations with magnetization along [100] and [001] direction are carried out using the frozen charge density produced from the collinear calculation, and then the K_i can be calculated based on the energy differences.[30] These two methods generally give consistent results for non-heavy metal systems, such as Fe/MgO and $Fe/MgAl_2O_4$.[31] However, according to a recent theoretical report, the results might be different for systems with heavy metals, such as Pt and Ir.[32] In this work, to avoid the failure of

perturbation theory, the first approach, that is, the fully self-consistent non-collinear SOC calculations were used for K_i.

III. RESULTS AND DISCUSSION

A. Uncapped MgO/Co_2FeAl

We began our study by investigating the interfacial magnetic anisotropy (K_i) and energetic properties of uncapped MgO/Co_2FeAl. Co_2FeAl has a cubic crystal structure ($L2_1$) with a space group No.225 $Fm\bar{3}m$.[11,33] The calculated lattice constants of bulk Co_2FeAl and MgO are 5.697 and 4.215 Å, respectively, close to their experimental values 5.730 and 4.211 Å.[33,34] To match the lattice constant of MgO substrate, a 45° rotation along [001] direction was made on the conventional lattice structure of Co_2FeAl, which yields a lattice mismatch of −4.4%. The negative sign here indicates that the Co_2FeAl film undergoes a tensile strain from the MgO substrate. In principle, there are four types of MgO/Co_2FeAl slab-based heterostructure models, with all the possible combinations between the two types of MgO/Co_2FeAl interfaces (MgO/Co_2 and MgO/FeAl interfaces) and two types of Co_2FeAl surfaces (with Co_2 and FeAl terminations), as shown in Fig. 1. The layers in the Co_2FeAl film from the MgO/Co_2FeAl interface to the Co_2FeAl surface are labeled as FL-I to FL-VIII, respectively. For convenience, the heterostructure model consisting of MgO/Co_2 interface and FeAl-terminated surface is referred to as MgO/Co_2...FeAl, along with the other three models, MgO/Co_2...Co_2, MgO/FeAl...Co_2, and MgO/FeAl...FeAl.

In each model, Co_2FeAl film was built on the MgO substrate with a thickness of five monolayers along [001] direction, and a thickness of more than 15 Å vacuum was added on the film to avoid the interaction between images in the periodic lattice. Our test calculations show that increasing the thickness of MgO monolayers more than five has no effects on the magnetic anisotropy, which is consistent with the prior computational study,[21] see Fig. S2 in the Supporting Information.[28] It is realized that, however, when the MgO was grown on the ferromagnetic Co_2FeAl as over-layers, its thickness could be a crucial factor that influence the magnetic anisotropy of MgO/Co_2FeAl system according to a recent experimental study.[35]

TABLE I. Total K_i values of uncapped MgO/Co_2FeAl system with different terminations

Structure	K_i (mJ/m^2)
MgO/Co_2...FeAl	0.60
MgO/Co_2...Co_2	1.28
MgO/FeAl...Co_2	0.12
MgO/FeAl...FeAl	-1.13

The K_i as a function of the thickness of Co_2FeAl film (number of layers) was studied for the four types of heterostructure models, MgO/Co_2...FeAl, MgO/Co_2...Co_2, MgO/FeAl...Co_2, and MgO/FeAl...FeAl. Our calculations show that the calculated K_i generally tends to be saturated when the number of Co_2FeAl layers is larger than five for all the types of heterostructure models, as shown in the Fig. S3 of Supporting Information.[28] This implies there exists a range of the film thickness to produce the desired perpendicular magnetic anisotropy. In fact, it was experimentally reported that the critical thickness for Co_2FeAl film to maintain out-of-plane K_i was around 1.1 nm after annealing at 300°C.[10,36] Therefore, in this work, we choose seven layers (the thickness of Co_2FeAl film is about 0.8 nm) for MgO/Co_2...FeAl and MgO/FeAl...Co_2 system, and eight layers (about 1 nm) for MgO/FeAl...Co_2 and MgO/FeAl...FeAl system to build up the uncapped MgO/Co_2FeAl models. Additionally, it is worth noting that the MgO/FeAl...FeAl model has a positive K_i (with an easy magnetization axis along out-of-plane direction) when the Co_2FeAl film is ultra thin (one layer), and the K_i becomes negative (with an easy magnetization axis along in-plane direction) for multilayers of Co_2FeAl film. The calculated K_i of MgO/Co_2FeAl model with the designated film thickness are 0.60 mJ/m^2 for MgO/Co_2...FeAl, 1.28 mJ/m^2 for MgO/Co_2...Co_2, 0.12 mJ/m^2 for MgO/FeAl...Co_2, and -1.13 mJ/m^2 for MgO/FeAl...FeAl, as listed in Table I. Our calculated K_i of 1.28 mJ/m^2 for MgO/Co_2...Co_2 structure is in good agreement with experimental values of 1.04 mJ/m^2[10] and 1.14 mJ/m^2[17], and is also well consistent with a recent DFT calculation of 1.31 mJ/m^2.[21]

The effective anisotropy for the MgO/Co_2...Co_2 model was estimated using the equation:[37,38]

$$K_{\text{eff}} t_{\text{eff}} = K_i - \frac{1}{2}\mu_0 M_s^2 t_{\text{eff}} \quad (1)$$

where K_{eff} is the effective anisotropy per unit volume, t_{eff} is the thickness of the ferromagnetic layer, μ_0 is the magnetic constant, and M_s is the saturation magnetization per unit volume. The term $\frac{1}{2}\mu_0 M_s^2$ represents demagnetizing energy per unit volume. In our calculations, the total magnetization for MgO/Co_2...Co_2 is 17.15 μ_B, and the effective thickness is 7.944 Å. Accordingly, the saturation magnetization M_s can be estimated to be 1127 emu/cm^3, which is close to the experimental value of 1140 emu/cm^3.[17] The term $\frac{1}{2}\mu_0 M_s^2 t_{\text{eff}}$ can be estimated to be around 0.63 mJ/m^2, which is much less than the K_i considered in this study. Therefore, it is reasonable to conclude that the effective anisotropy still favors the PMA in the MgO/Co_2...Co_2 model.

To understand the origin of the K_i, we calculated layer-resolved K_i for the four types of models, which clearly shows the atomic contributions to the K_i, see Fig. 2. The layer-resolved K_i was calculated based on the energy difference in non-collinear calculations projected for the atom in each layer. As one can see, Al atom barely

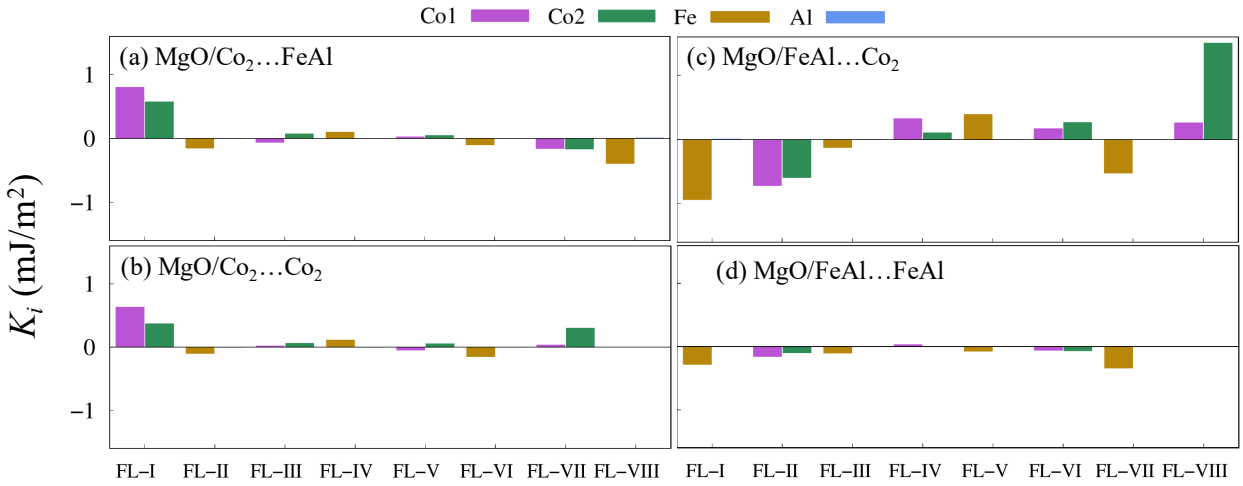

FIG. 2. Calculated layer-resolved K_i values of different atoms for (a) MgO/Co_2...FeAl, (b) MgO/Co_2...Co_2, (c) MgO/FeAl...Co_2, (d) MgO/FeAl...FeAl structures. Label FL-I to FL-VIII corresponds with the layers from MgO/Co_2FeAl interface to Co_2FeAl surface. The purple and green bars represent two different Co atoms in the same layer, while the green and blue bars indicate Fe and Al atom, respectively in the same layer.

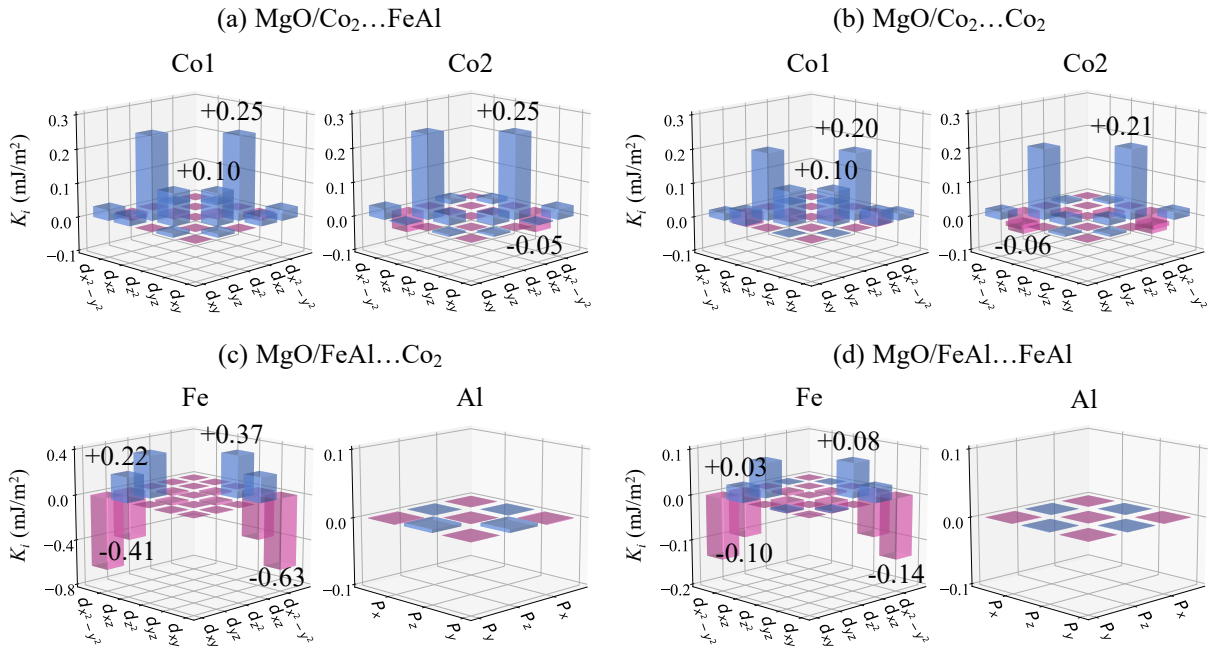

FIG. 3. Calculated atomic-resolved K_i contributions from different orbital hybridizations. (a) and (b) are d-orbital hybridization of interfacial Co atoms in MgO/Co_2...FeAl and MgO/Co_2...Co_2 structure, respectively. (c) and (d) are d-orbital hybridization of interfacial Fe atom and p-orbital hybridization of interfacial Al atom in MgO/FeAl...Co_2 and MgO/FeAl...FeAl structure, respectively.

contributes to K_i, however, Co and Fe atoms play an important role in producing the K_i. For the models MgO/Co_2...FeAl and MgO/Co_2...Co_2, the two interfacial Co atoms in the FL-I layer contribute most of the out-of-plane K_i, resulting in a positive total K_i of 0.60 mJ/m^2 and 1.28 mJ/m^2, respectively, see Fig. 2a and 2b. On the contrary, for the models MgO/FeAl...Co_2 and MgO/FeAl...FeAl, the interfacial Fe atoms (FL-I) and Co atoms (IF-II) cause negative K_i, which explains the relatively low K_i (0.12 mJ/m^2) in MgO/FeAl...Co_2 and even negative K_i (-1.13 mJ/m^2) in MgO/FeAl...FeAl. In the model MgO/FeAl...Co_2, the surface Co atoms in the layer FL-VIII cause a large out-of-plane K_i, cancels out the in-plane K_i, and leads to a total positive but low K_i, see Fig. 2c. In the model MgO/FeAl...FeAl, almost all the layers contribute in-plane K_i, leading to a to-

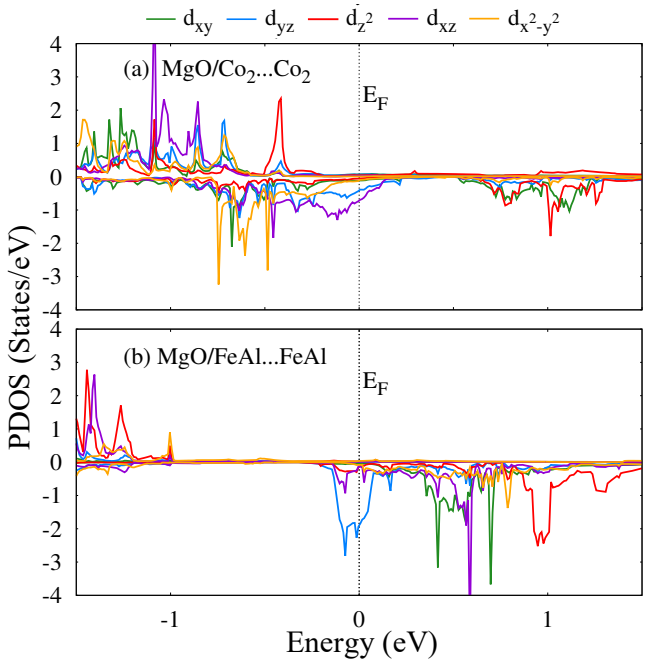

FIG. 4. Calculated projected density of states (PDOS) of d orbitals for (a) Co2 atom at MgO/Co_2 interface in the $MgO/Co_2...Co_2$ model and (b) Fe atom at MgO/FeAl interface in the MgO/FeAl...FeAl model.

tal negative K_i, see Fig. 2d. Interestingly, although the models MgO/FeAl...Co_2 and MgO/FeAl...FeAl share the same interface, *i.e.*, MgO/FeAl, their layer-resolved K_i are significantly different, which may be attributed to the structure symmetry of the Co_2FeAl layer.[2] That is, one additional Co_2 layer in the MgO/FeAl...Co_2 model can significantly change the layer-resolved K_i compared to the model MgO/FeAl...FeAl in which the ferromagnetic Co_2FeAl layer is symmetrical. In short, our calculations reveal that the MgO/Co_2 interface produces the out-of-plane K_i while the MgO/FeAl interface produces in-plane K_i.

To further understand the microscopic origin of K_i, we calculated orbital-resolved K_i for the interfacial atoms, *i.e.*, Co $3d$ orbitals at the MgO/Co_2 interface and Fe $3d$ and Al $3p$ orbitals at MgO/FeAl interface, as shown in Fig. 3. For the models MgO/Co_2...FeAl and $MgO/Co_2...Co_2$, the out-of-plane K_i mainly comes from hybridization between d_{xz} and d_{yz} orbitals of the interfacial Co atoms at the MgO/Co_2 interface, around 0.25 mJ/m^2 and 0.20 mJ/m^2, respectively, see Fig. 3a and 3b. The hybridization between d_{z^2} and d_{yz} also contributes to the out-of-plane K_i in both structures, however, the magnitude is much small. For the models MgO/FeAl...FeAl and MgO/FeAl...Co_2, d_{xz} and d_{yz} orbital hybridization of Fe atoms at MgO/FeAl interface also yields out-of-plane K_i, about 0.37 mJ/m^{2}and 0.08 mJ/m^2, respectively, as shown in Fig. 3c and 3d. However, the orbital hybridization between $d_{x^2-y^2}$ and d_{xy}, and $d_{x^2-y^2}$ and d_{yz}, leads to an in-plane (negative) K_i and the resulting relatively low out-of-plane total K_i for the model MgO/FeAl...Co_2 and even negative K_i for MgO/FeAl...FeAl model.

The SOC effects on the magnetic anisotropy energy (MAE) can be derived from the second perturbation theory:[39]

$$\begin{aligned} MAE \approx &(\xi)^2 \sum_{o^\downarrow,u^\downarrow} \frac{|\langle o^\downarrow|L_z|u^\downarrow\rangle|^2 - |\langle o^\downarrow|L_x|u^\downarrow\rangle|^2}{\epsilon_{u^\downarrow} - \epsilon_{o^\downarrow}} \\ &+(\xi)^2 \sum_{o^\uparrow,u^\downarrow} \frac{|\langle o^\uparrow|L_x|u^\downarrow\rangle|^2 - |\langle o^\uparrow|L_z|u^\downarrow\rangle|^2}{\epsilon_{u^\downarrow} - \epsilon_{o^\uparrow}} \end{aligned} \quad (2)$$

where ξ is the SOC constant; $o^\uparrow(u^\uparrow)$ and $o^\downarrow(u^\downarrow)$ denote the occupied (unoccupied) spin-up and spin-down eigenstates, respectively; $\epsilon_{o^\uparrow(u^\uparrow)}$ and $\epsilon_{o^\downarrow(u^\downarrow)}$ represent eigenvalues of occupied (unoccupied) spin-up and spin-down states, respectively; the $L_z(L_x)$ are the angular momentum operators. This theory has been used to successfully explain the K_i distribution of interfacial Fe over Brillouin zone in Fe/MgO,[40,41] Fe/$CuInSe_2$,[42] and Fe/$MgAl_2O_4$.[31] For a system with a large spin polarization like MgO/Co_2FeAl, the coupling effects from the opposite spin channel can be neglected, and thus the MAE is mainly determined by the coupling between the occupied and unoccupied spin-down states near the Fermi level.[39] In this case, the orbital coupling between occupied and unoccupied states yields a positive K_i if these states share the same quantum number $|m|$, and the coupling yields a negative K_i if the quantum numbers of these states differ by one. To be specific, the orbital coupling between occupied and unoccupied spin-down states, *i.e.*, d_{xy} and $d_{x^2-y^2}$ (with $|m| = 2$), and between d_{xz} and d_{yz} (with $|m| = 1$) will contribute to a positive K_i.[37,43]

To qualitatively understand how the orbital hybridization determines magnetic anisotropy, we calculated projected density of states (PDOS) of d orbitals for the interfacial Co atom in $MgO/Co_2...Co_2$ model and for the interfacial Fe atom in MgO/FeAl...FeAl model, as shown in Fig. 4a and 4b, respectively. For the $MgO/Co_2...Co_2$ model, spin-down d_{yz} and d_{xz} orbitals contribute both occupied and unoccupied states in the very vicinity ($\pm$0.1 eV) of the Fermi level, and hence their orbital coupling between occupied and unoccupied states leads to an out-of-plane K_i. This is also consistent with the orbital-resolved K_i in Fig. 3b. For the MgO/FeAl...FeAl model, the orbital coupling between occupied d_{xz} and unoccupied d_{yz} states leads to positive K_i, as shown in the orbital-resolved K_i in Fig. 3d, similar to the case of $MgO/Co_2...Co_2$ model. However, as discussed below from the k-space-resolved MAE, the orbital coupling between d_{yz} (d_{xz}) and $d_{x^2-y^2}$ states leads to negative K_i, thus resulting in a negative K_i in total.

To deeply understand the relationship between orbital hybridization and magnetic anisotropy, we further calculated k-space-resolved MAE projected on the two-dimensional interfacial Brillouin zone using a so-called

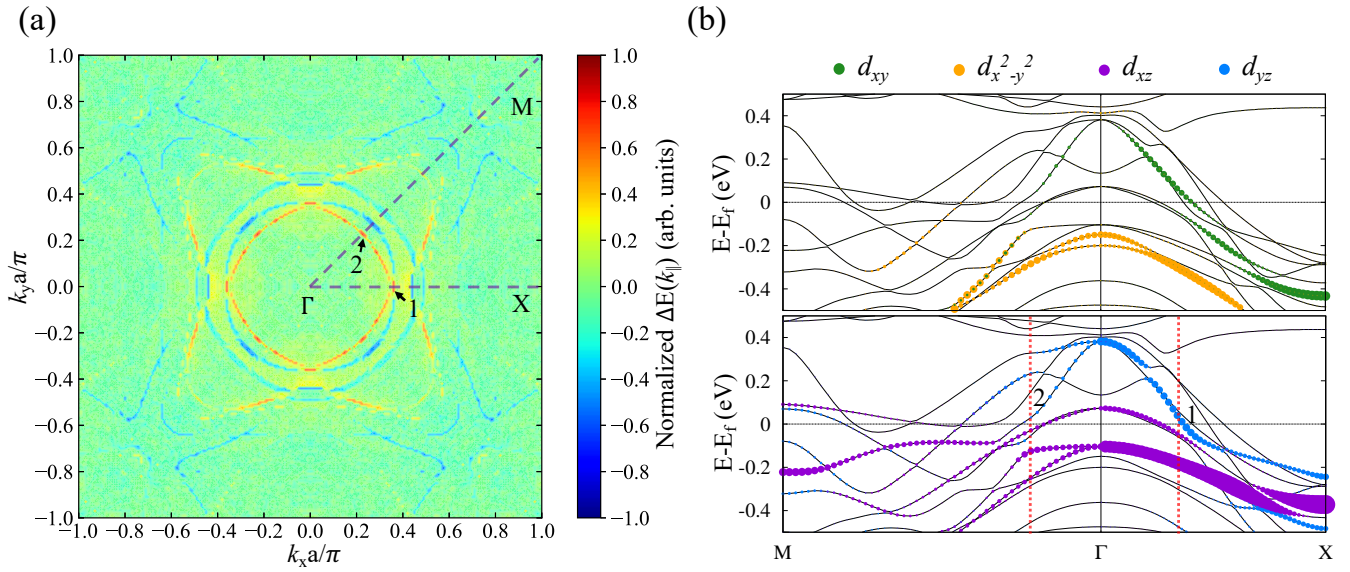

FIG. 5. The k-resolved MAE and d-orbital projected band structure for MgO/Co_2...Co_2 structure. (a) Distribution of MAE of interfacial Co atom (Co atom at MgO/Co_2 interface) in the 2D Brillouin zone. The MAE value was normalized to the maximum positive value of the 2D Brillouin zone. The red and blue colors represent out-of-plane and in-plane MAE, respectively. (b) d-orbital projected band structure of interfacial Co atom in spin-down states. The positions of vertical red dash lines 1 and 2 correspond to the out-of-plane MAE from coupling between d_{xz} and d_{yz} orbitals.

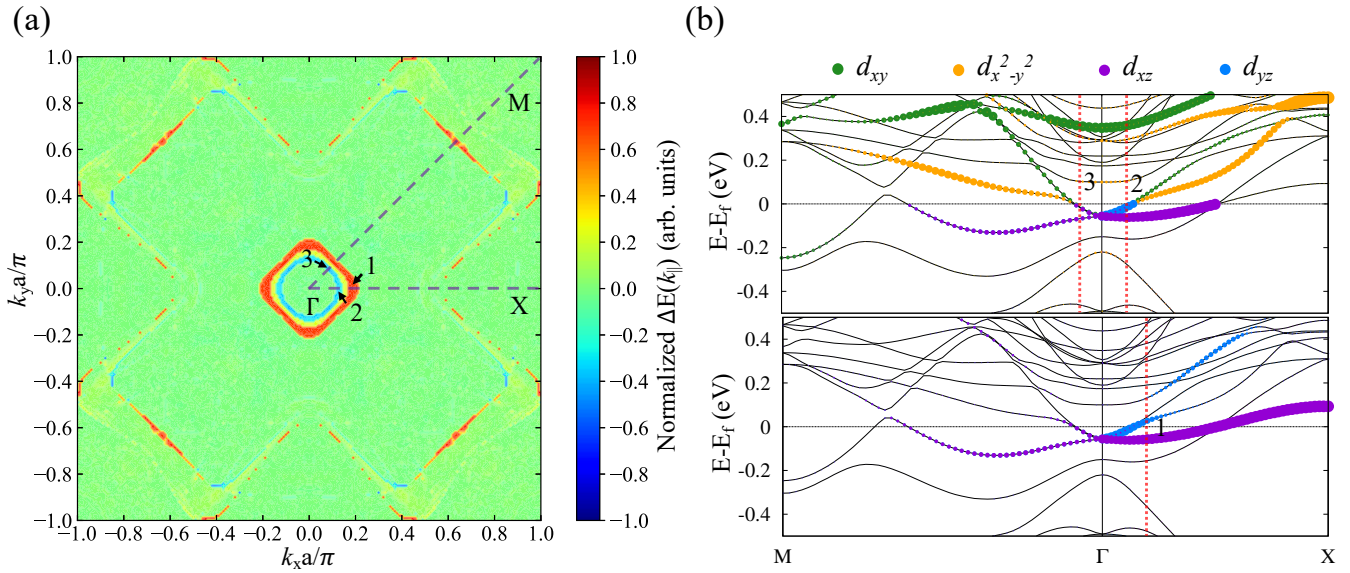

FIG. 6. The k-resolved MAE and d-orbital projected band structure for MgO/FeAl...FeAl structure. (a) Distribution of MAE of interfacial Fe atom (Fe atom at MgO/FeAl interface) in the 2D Brillouin zone. The MAE value was normalized to the maximum positive value of the 2D Brillouin zone. The red and blue colors represent out-of-plane and in-plane MAE, respectively. (b) d-orbital projected band structure of interfacial Fe atom in spin-down states. The position of vertical red dash line 1 corresponds to the out-of-plane MAE from coupling between d_{xz} and d_{yz} orbitals, and the positions of vertical red dash lines 2 and 3 correspond to the in-plane MAE from coupling between d_{yz} and $d_{x^2-y^2}$ orbitals and coupling between d_{xz} and $d_{x^2-y^2}$ orbitals.

"force theorem" approach[44], see Fig. 5a and 6a. The d-orbital projected band structures for the two models, MgO/Co_2...Co_2 and MgO/FeAl...FeAl, are also shown in Fig. 5b and 6b, respectively. For the MgO/Co_2...Co_2 model, as shown in Fig. 5a and 5b, its positive MAE at k-points 1 and 2 arises from the coupling between occupied and unoccupied spin-down states d_{xz} and d_{yz} along Γ-M and Γ-X, respectively. This conclusion is also in good agreement with our orbital-resolved K_i values for interfacial Co atoms in Fig. 3b. For MgO/FeAl...FeAl model,

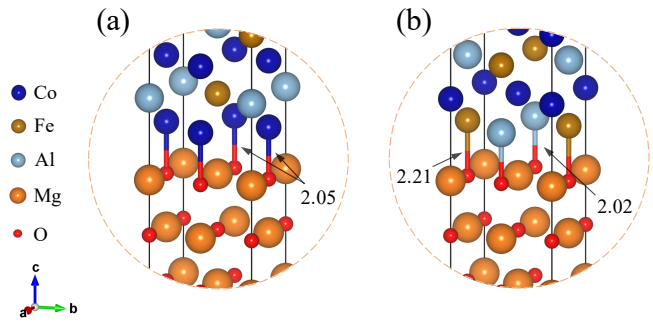

FIG. 7. Schematic illustration of interfacial bond length in the unit of Å at (a) MgO/Co_2 interface and (b) MgO/FeAl interface.

as shown in Fig. 6a and 6b, its positive MAE at k-point 1 arises from the coupling between occupied and unoccupied spin-down states d_{xz} and d_{yz} along Γ-X; while the negative MAE at k-points 2 and 3 comes from the coupling between occupied and unoccupied spin-down d_{yz} and $d_{x^2-y^2}$ orbitals along Γ-X and between d_{xz} and $d_{x^2-y^2}$ orbitals along Γ-M, respectively.

To evaluate relative interfacial thermal stability, we calculated cleavage energy of MgO/Co_2 and MgO/FeAl interfaces using the bulk heterostructure model of MgO/Co_2FeAl (without vacuum) based on the below equation:[45]

$$E_{cleav.} = (E_{slab}^{Co_2FeAl} + E_{slab}^{MgO} - E_{HS}^{MgO/Co_2FeAl})/2A \quad (3)$$

where $E_{slab}^{Co_2FeAl}$, E_{slab}^{MgO}, andE_{HS}^{MgO/Co_2FeAl} are the total energy of Co_2FeAl slab, MgO slab, and MgO/Co_2FeAl heterostructure, respectively. A is the in-plane interfacial area, and factor 2 in the denominator represents two symmetrical interfaces in the heterostructure model. The calculated cleavage energy was 117 meV/Å^2 for MgO/Co_2 interface and 82 meV/Å^2 for MgO/FeAl interface, indicating that the MgO/Co_2 interface is energetically more favorable than the MgO/FeAl interface. Accordingly, we can conclude that the MgO/Co_2 interface is more likely to be formed than the MgO/FeAl interface in the experiments. Considering the positive K_i at MgO/Co_2 interface and the negative (or close to zero) K_i at MgO/FeAl interface, this conclusion is also well consistent with the experimentally observed perpendicular magnetic anisotropy at the interface of MgO/Co_2FeAl.[10,17]

The relative thermal stability of the two interface models can be understood from the interfacial bond length and the resulting bond strength. The local geometrical structures of the two interface models are shown in Fig. 7. The two Co-O bonds at MgO/Co_2 interface are equivalent, with a bond length of 2.05 Å, while at MgO/FeAl interface, the relaxed Fe-O and Al-O bonds are different mainly because of the different atomic radii for Fe and Al, with a bond length of 2.21 Å and 2.02 Å, respectively. Accordingly, the relatively low cleavage energy at MgO/FeAl interface can be attributed to the unmatched Fe-O and Al-O bond length and the resulting relatively weak bond strength, while the highly uniform interfacial structure (equivalent Co-O bonds) at the MgO/Co_2 interface leads to relatively high cleavage energy. Note that the unmatched bond strength between Fe-O and Al-O bonds can also be proven from the Bader charge analysis for the interfacial O atoms.[46]

B. Capped MgO/Co_2FeAl

In this section, we studied the influence of adding capping layers on the interfacial magnetic anisotropy of MgO/Co_2FeAl. A total number of 26 metal elements including $3d$ (Ti, V, Cr, Mn, Fe, Ni, and Cu), $4d$ (Zr, Nb, Mo, Tc, Ru, Rh, Pd, and Ag), $5d$ (Hf, Ta, W, Re, Os, Ir, Pt, and Au) TMs, and $6p$ (Tl, Pb, and Bi) metals were considered as capping layers. This is based on the consideration that these elements have a relatively large spin-orbit coupling (SOC) interaction that is likely to be capable of tuning the interfacial magnetic anisotropy.[7] The Co element is not included due to the large lattice mismatch between FCC-Co and MgO substrate (∼16 %). Since our calculations show that the MgO/Co_2 interface is energetically more favorable than the MgO/FeAl interface, here we only considered MgO/Co_2...FeAl and MgO/Co_2...Co_2 models. We built the capped-MgO/Co_2FeAl by adding

TABLE II. Summary of total K_i values of selected capping elements with lattice mismatch (f) smaller than 7%. The lattice mismatch is defined as $f = (a_f - a_s)/a_s$, where a_s and a_f are the lattice constant of substrate and film, respectively.

X	f(%)	K_i (mJ/m^2)	
		MgO/Co_2...FeAl/X	MgO/Co_2...Co_2/X
Ti	-2.5	0.71	1.00
V	0.4	0.98	0.87
Cr	-4.4	1.20	1.22
Mn	-6.1	0.73	0.48
Fe	-4.4	2.59	2.13
Ni	-6.4	-0.37	1.79
Cu	-3.6	1.21	1.22
Nb	0.4	0.58	1.18
Mo	-4.8	1.37	0.93
Pd	-6.2	1.86	0.60
Ag	-1.3	1.15	1.23
Hf	6.3	1.67	0.93
Ta	0.3	-0.72	0.63
W	6.2	4.90	2.46
Re	-6.9	0.27	-1.63
Pt	-5.6	0.56	-1.37
Au	-1.0	1.82	1.33
Tl (I)	-6.0	-1.76	2.12
Tl (II)			2.14
Pb (I)	-5.0	-0.35	2.01
Pb (II)			2.29
Bi (I)	-5.4	0.40	0.13
Bi (II)			2.08

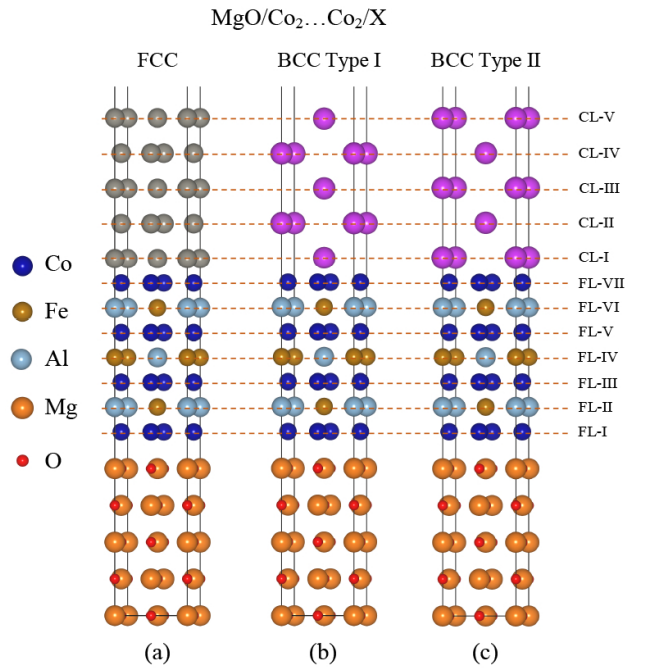

FIG. 8. Schematic crystal structures of capped $MgO/Co_2...Co_2$ heterostructure with (a) FCC structure capping layer, (b) BCC type I structure capping layer, and (c) BCC type II structure capping layer.

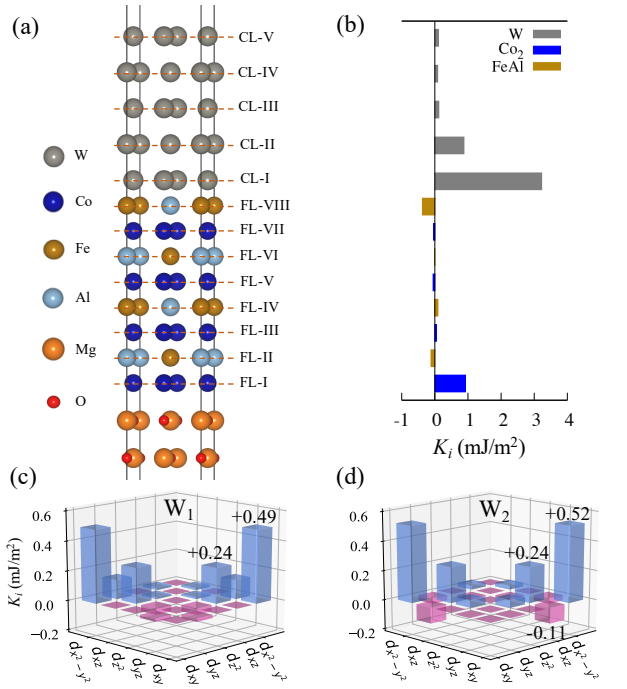

FIG. 9. (a) Schematic crystal structure of W-capped $MgO/Co_2...FeAl$ ($MgO/Co_2...FeAl/W$) (b) layer-resolved K_i value of $MgO/Co_2...FeAl/W$ (c) and (d) K_i contributions from different d orbital hybridizations at the interfacial atoms of W1 and W2 of $MgO/Co_2...FeAl/W$.

the FCC-type or BCC-type structures of these metal elements on top of the Co_2FeAl film while maintaining the thickness of vacuum around 15 Å, see Fig. 8. It is noted that, for the $MgO/Co_2...Co_2$ model, there are two types of interfacial structures between Co_2FeAl film and BCC-type capping layer (including Tl, Pb, and Bi), and one type of interfacial structure between the Co_2FeAl film and FCC-type capping layer, as shown in the schematic crystal structures in Fig. 8. The layers of capping elemental compound are labeled as CL-I, CL-II, CL-III, CL-IV, and CL-V, respectively. In the case of V-, Cr-, Mn-, Fe-, Ni-, Cu-, and W-capped structures, to produce the best lattice match, a 45° rotation along [001] direction was made on the conventional bulk structure of BCC-type V, Cr, Mn, Fe, Ni, Cu, and W, leading to only one type of interfacial structure. By taking W-capped MgO/Co_2FeAl as one example, we also studied the total K_i as a function of the number of capping layers, as shown in the Fig. S2 of Supporting Information.[28] Our calculations show that the K_i of the system with an odd number of capping layers (3, 5, and 7) is generally larger than that with an even number (4 and 6), and in spite of this, the K_i still tends to be saturated as the number of capping layers is larger than five.

Table II shows the summary of K_i values of selected capped MgO/Co_2FeAl systems that have a lattice mismatch (between Co_2FeAl and capping elemental bulk structure) less than 7%. The detailed results of all the 26 capped models are shown in the Table S1 of Supporting Information.[28] It shows that Fe-, Mo-, Pd-, Hf-, W-, and Au-capped $MgO/Co_2...FeAl$ structures show a larger K_i of 2.59, 1.37, 1.86, 1.67, 4.90, and 1.82 mJ/m^2 than the uncapped structure. The Tl-, Pb-, and Bi-capped MgO/Co_2FeAl structures with a type II structure also exhibit a large K_i of 2.14, 2.29, and 2.08 mJ/m^2. It is especially worth mentioning that W capping leads to a giant K_i value of 4.90 mJ/m^2 in $MgO/Co_2...FeAl/W$ structure and a K_i of 2.46 mJ/m^2 in the $MgO/Co_2...Co_2/W$ structure. Interestingly, prior experimental and computational studies indicated that W can also improve K_i in the Fe/W/MgO[7,47] and MgO/CoFeB/W/CoFeB/MgO[48] systems in which a thin W interface layer was inserted as doping. Additionally, our calculation for $MgO/Co_2...Co_2/Ta$ yield a K_i value of 0.63 mJ/m^2, which is in good agreement with the experimental value of 0.67 mJ/m^2.[23] To elucidate the origin of the giant K_i in $MgO/Co_2...FeAl/W$ structure, we calculated its layer-resolved K_i and atomic orbital-resolved K_i in Fig. 9. It clearly shows that the large K_i of $MgO/Co_2...FeAl/W$ is mainly contributed by the interfacial W atoms at the CL-I (3.22 mJ/m^2) and CL-II (0.88 mJ/m^2) layers. The K_i from the interfacial Co atoms of Co_2FeAl is almost the same with that in the uncapped MgO/Co_2FeAl model, suggesting that the W capping layers has no significant influence on the magnetic anisotropy of the Co_2FeAl film but does enhance the total K_i of the $MgO/Co_2...FeAl/W$ system. The orbital-

resolved K_i of the two interfacial W atoms at CL-I layer were plotted in Fig. 9c and 9d. It shows that the out-of-plane K_i largely comes from the d orbital hybridization between $d_{x^2-y^2}$ and d_{xy} (around 0.50 mJ/m^2), and between d_{xz} and d_{yz} (0.24 mJ/m^2) in both W atoms.

IV. CONCLUSION

In conclusion, we have systematically investigated the interfacial magnetic and energetic properties in the MgO/Co_2FeAl heterostructure by modeling four types of interfacial models using first-principles calculations. Our results show that MgO/Co_2 interface can produce out-of-plane K_i while MgO/FeAl interface can produce in-plane K_i, and the former interface is energetically more favorable than the later one and thus is likely to be formed practically. The calculated K_i of 1.28 mJ/m^2 in the MgO/Co_2...Co_2 structure is well consistent with the experimental value. In addition, the influence of 26 capping layers on the interfacial magnetic anisotropy was explored. It is found that Fe- and W-capping can significantly enhance the interfacial K_i in the MgO/Co_2FeAl, and particularly, a giant K_i of 4.90 mJ/m^2 can be achieved in the W-capped model. This work reveals the atomistic origin of the large perpendicular magnetic anisotropy at MgO/CO_2FeAl interface and offers insights to tune interfacial K_i via adding capping layers in the MgO/Co_2FeAl.

V. ACKNOWLEDGMENT

This work was supported by Academic Senate General Campus Research Grant Committee at University of California San Diego, National Science Foundation under award number ACI-1550404, and Vannevar Bush Faculty Fellowship program sponsored by the Basic Research Office of the Assistant Secretary of Defense for Research and Engineering (under the Office of Naval Research grant N00014-16-1-2569). This work used the Extreme Science and Engineering Discovery Environment (XSEDE), which is supported by National Science Foundation grant number ACI-1548562.

* kesong@ucsd.edu

[1] Y. Huai, AAPPS bulletin **18**, 33 (2008).
[2] A. Khvalkovskiy, D. Apalkov, S. Watts, R. Chepulskii, R. Beach, A. Ong, X. Tang, A. Driskill-Smith, W. Butler, P. Visscher, *et al.*, J. Phys. D: Appl. Phys. **46**, 074001 (2013).
[3] A. Moser, K. Takano, D. T. Margulies, M. Albrecht, Y. Sonobe, Y. Ikeda, S. Sun, and E. E. Fullerton, J. Phys. D: Appl. Phys. **35**, R157 (2002).
[4] S. Yuasa, T. Nagahama, A. Fukushima, Y. Suzuki, and K. Ando, Nat. Mater. **3**, 868 (2004).
[5] S. Ikeda, K. Miura, H. Yamamoto, K. Mizunuma, H. D. Gan, M. Endo, S. Kanai, J. Hayakawa, F. Matsukura, and H. Ohno, Nat. Mater. **9**, 721 (2010).
[6] S. Peng, D. Zhu, J. Zhou, B. Zhang, A. Cao, M. Wang, W. Cai, K. Cao, and W. Zhao, Adv. Electron. Mater. , 1900134 (2019).
[7] S. Nazir, S. Jiang, J. Cheng, and K. Yang, Appl. Phys. Lett. **114**, 072407 (2019).
[8] S. Peng, W. Kang, M. Wang, K. Cao, X. Zhao, L. Wang, Y. Zhang, Y. Zhang, Y. Zhou, K. L. Wang, and W. Zhao, IEEE Magn. Lett. **8**, 1 (2017).
[9] V. W. Guo, B. Lu, X. Wu, G. Ju, B. Valcu, and D. Weller, J. Appl. Phys. **99**, 08E918 (2006).
[10] Z. Wen, H. Sukegawa, S. Mitani, and K. Inomata, Appl. Phys. Lett. **98**, 242507 (2011).
[11] M. Gabor, T. Petrisor Jr, C. Tiusan, M. Hehn, and T. Petrisor, Phys. Rev. B **84**, 134413 (2011).
[12] A. Kumar, F. Pan, S. Husain, S. Akansel, R. Brucas, L. Bergqvist, S. Chaudhary, and P. Svedlindh, Phys. Rev. B **96**, 224425 (2017).
[13] S. Mizukami, D. Watanabe, M. Oogane, Y. Ando, Y. Miura, M. Shirai, and T. Miyazaki, J. Appl. Phys. **105**, 07D306 (2009).
[14] W. Wang, E. Liu, M. Kodzuka, H. Sukegawa, M. Wojcik, E. Jedryka, G. Wu, K. Inomata, S. Mitani, and K. Hono, Phys. Rev. B **81**, 140402 (2010).
[15] X. Li, S. Yin, Y. Liu, D. Zhang, X. Xu, J. Miao, and Y. Jiang, Appl. Phys. Express **4**, 043006 (2011).
[16] M. Belmeguenai, H. Tuzcuoglu, M. S. Gabor, T. Petrisor, C. Tiusan, D. Berling, F. Zighem, T. Chauveau, S. M. Chérif, and P. Moch, Phys. Rev. B **87**, 184431 (2013).
[17] A. Conca, A. Niesen, G. Reiss, and B. Hillebrands, J. Phys. D: Appl. Phys. **51**, 165303 (2018).
[18] J. Okabayashi, H. Sukegawa, Z. Wen, K. Inomata, and S. Mitani, Appl. Phys. Lett. **103**, 102402 (2013).
[19] Z. Wen, J. P. Hadorn, J. Okabayashi, H. Sukegawa, T. Ohkubo, K. Inomata, S. Mitani, and K. Hono, Appl. Phys. Express **10**, 013003 (2017).
[20] Z. Bai, L. Shen, Y. Cai, Q. Wu, M. Zeng, G. Han, and Y. P. Feng, New J. Phys. **16**, 103033 (2014).
[21] R. Vadapoo, A. Hallal, H. Yang, and M. Chshiev, Phys. Rev. B **94**, 104418 (2016).
[22] M. Belmeguenai, M. Gabor, T. Petrisor Jr, F. Zighem, S. Chérif, and C. Tiusan, J. Appl. Phys. **117**, 023906 (2015).
[23] M. S. Gabor, T. Petrisor, C. Tiusan, and T. Petrisor, J. Appl. Phys. **114**, 063905 (2013).
[24] G. Kresse and J. Furthmüller, Comput. Mater. Sci. **6**, 15 (1996).
[25] G. Kresse and J. Furthmüller, Phys. Rev. B **54**, 11169 (1996).
[26] G. Kresse and D. Joubert, Phys. Rev. B **59**, 1758 (1999).
[27] J. P. Perdew, K. Burke, and M. Ernzerhof, Phys. Rev. Lett. **77**, 3865 (1996).
[28] See Supplemental Material at [URL will be inserted by publisher] for the convergence test results for K_i and cleavage energy and the calculated K_i for all the 26 capped MgO/Co_2FeAl models.

[29] P. E. Blöchl, O. Jepsen, and O. K. Andersen, Phys. Rev. B **49**, 16223 (1994).
[30] S. Steiner, S. Khmelevskyi, M. Marsmann, and G. Kresse, Phys. Rev. B **93**, 224425 (2016).
[31] K. Masuda and Y. Miura, Phys. Rev. B **98**, 224421 (2018).
[32] S. Kwon, Q. Sun, F. Mahfouzi, K. L. Wang, P. K. Amiri, and N. Kioussis, Phys. Rev. A **12**, 044075 (2019).
[33] K. v. Buschow, P. Van Engen, and R. Jongebreur, J. Magn. Magn. Mater. **38**, 1 (1983).
[34] M. Boiocchi, F. Caucia, M. Merli, D. Prella, and L. Ungaretti, Eur. J. Mineral. **13**, 871 (2001).
[35] S. Lakshmanan, M. R. Muthuvel, P. Delhibabu, and H. Annal Therese, Phys. Status Solidi A **215**, 1800316 (2018).
[36] H. Sukegawa, Z. Wen, S. Kasai, K. Inomata, and S. Mitani, Spin **4**, 1440023 (2014).
[37] B. Dieny and M. Chshiev, Rev. Mod. Phys. **89**, 025008 (2017).
[38] K. Masuda, S. Kasai, Y. Miura, and K. Hono, Phys. Rev. B **96**, 174401 (2017).
[39] D.-s. Wang, R. Wu, and A. J. Freeman, Phys. Rev. B **47**, 14932 (1993).
[40] K. Nakamura, T. Akiyama, T. Ito, M. Weinert, and A. J. Freeman, Phys. Rev. B **81**, 220409 (2010).
[41] S. Kwon, P.-V. Ong, Q. Sun, F. Mahfouzi, X. Li, K. L. Wang, Y. Kato, H. Yoda, P. K. Amiri, and N. Kioussis, Phys. Rev. B **99**, 064434 (2019).
[42] K. Masuda, S. Kasai, Y. Miura, and K. Hono, Phys. Rev. B **96**, 174401 (2017).
[43] X. Chen, S. Zhang, B. Liu, F. Hu, B. Shen, and J. Sun, Phys. Rev. B **100**, 144413 (2019).
[44] G. Daalderop, P. Kelly, and M. Schuurmans, Phys. Rev. B **41**, 11919 (1990).
[45] S. Nazir, M. Behtash, and K. Yang, J. Appl. Phys. **117**, 115305 (2015).
[46] W. Tang, E. Sanville, and G. Henkelman, J. Phys.: Condens. Matter **21**, 084204 (2009).
[47] Y. Iida, Q. Xiang, J. Okabayashi, T. Scheike, H. Sukegawa, and S. Mitani, J. Phys. D: Appl. Phys. **53**, 124001 (2019).
[48] J.-H. Kim, J.-B. Lee, G.-G. An, S.-M. Yang, W.-S. Chung, H.-S. Park, and J.-P. Hong, Sci. Rep. **5**, 16903 (2015).